AD-A092 709 NAVAL RESEARCH LAB WASHINGTON DC F/G 17/4
COMPARISON OF DETECTORS IN THE PRESENCE OF SIDELOBE JAMMING.(U)
OCT 80 G V TRUNK
UNCLASSIFIED NRL-8449 NL

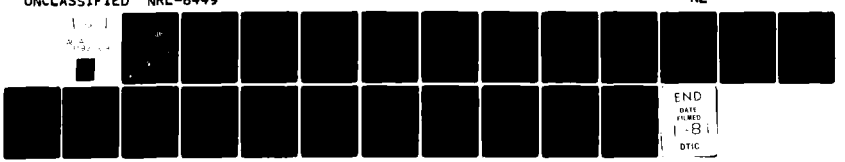

END
DATE FILMED
1-81
DTIC

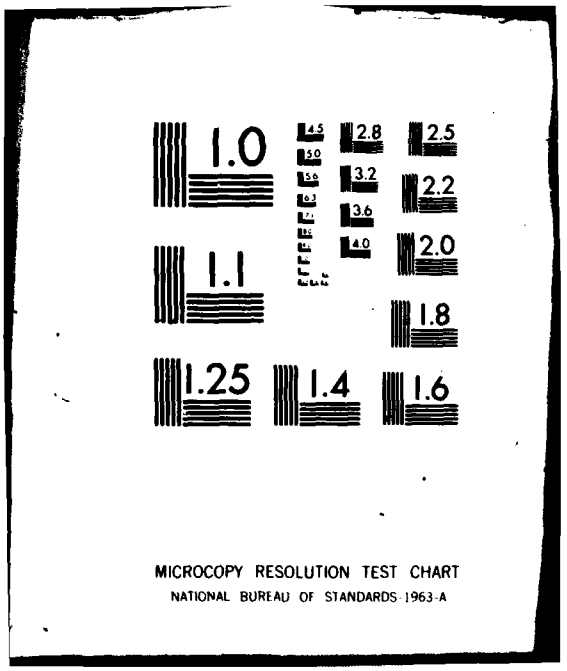
1.0
1.1
1.25
1.4
1.6
1.8
2.0
2.2
2.5
2.8
3.2
3.6
4.0
4.5
5.0
5.6
6.3
MICROCOPY RESOLUTION TEST CHART
NATIONAL BUREAU OF STANDARDS-1963-A

NRL Report 8449

Comparison of Detectors in the Presence of Sidelobe Jamming

(12)

G. V. Trunk

Radar Analysis Branch
Radar Division

LEVEL II

October 23, 1980

NAVAL RESEARCH LABORATORY
Washington, D.C.

NRL Report 8449

Comparison of Detectors in the Presence of Sidelobe Jamming

G. V. Trunk

Radar Analysis Branch
Radar Division

October 23, 1980

NAVAL RESEARCH LABORATORY
Washington, D.C.

SECURITY CLASSIFICATION OF THIS PAGE (When Data Entered)

REPORT DOCUMENTATION PAGE

READ INSTRUCTIONS BEFORE COMPLETING FORM

1. REPORT NUMBER: NRL Report 8449	2. GOVT ACCESSION NO.
3. RECIPIENT'S CATALOG NUMBER	
4. TITLE (and Subtitle): COMPARISON OF DETECTORS IN THE PRESENCE OF SIDELOBE JAMMING	5. TYPE OF REPORT & PERIOD COVERED: Interim report on a continuing NRL problem
	6. PERFORMING ORG. REPORT NUMBER
7. AUTHOR(s): G. V. Trunk	8. CONTRACT OR GRANT NUMBER(s)
9. PERFORMING ORGANIZATION NAME AND ADDRESS: Naval Research Laboratory, Washington, DC 20375	10. PROGRAM ELEMENT, PROJECT, TASK AREA & WORK UNIT NUMBERS: 61153N; RR-021-05-41; NRL Problem 53-0626-0
11. CONTROLLING OFFICE NAME AND ADDRESS: Department of the Navy, Office of Naval Research, Arlington, VA 22217	12. REPORT DATE: October 1980
	13. NUMBER OF PAGES: 22
14. MONITORING AGENCY NAME & ADDRESS (if different from Controlling Office)	15. SECURITY CLASS. (of this report): UNCLASSIFIED
	15a. DECLASSIFICATION/DOWNGRADING SCHEDULE

16. DISTRIBUTION STATEMENT (of this Report)

Approved for public release; distribution unlimited.

17. DISTRIBUTION STATEMENT (of the abstract entered in Block 20, if different from Report)

18. SUPPLEMENTARY NOTES

19. KEY WORDS (Continue on reverse side if necessary and identify by block number)

Detection
Cell-average CFAR
Sidelobe jamming

20. ABSTRACT (Continue on reverse side if necessary and identify by block number)

The problem of detecting targets in the presence of sidelobe jamming using noncoherent detectors is considered. It is shown that the ratio detector has better performance than the normally used cell-average CFAR. Tests using recorded jamming data confirm the theoretical advantage of the ratio detector.

DD FORM 1 JAN 73 1473 EDITION OF 1 NOV 65 IS OBSOLETE
S/N 0102-014-6601

SECURITY CLASSIFICATION OF THIS PAGE (When Data Entered)

CONTENTS

COMPARISON OF DETECTORS IN THE PRESENCE OF SIDELOBE JAMMING

INTRODUCTION

Automatic detection systems have been designed with the philosophy that they will suffer a small detection-sensitivity loss in thermal noise and at the same time the number of undesirable detections (i.e., noise false alarms and clutter residues) will be limited so that the automatic tracking system will not be overloaded. In this report, the design of an automatic detector will be considered for the case of sidelobe noise jamming. The basic idea is to configure the detector so that targets can be detected when the jammer is in sidelobe nulls of the antenna.

MATHEMATICAL FORMULATION

If the jamming is white Gaussian noise, the density of the ith output pulse x_i from an envelope detector is

$$p(x_i|A_i) = \frac{x_i}{\sigma_i^2} \exp\left[-\left(x_i^2 + A_i^2\right)/2\sigma_i^2\right] I_0\left(A_i x_i/\sigma_i^2\right), \tag{1}$$

where A_i is the signal amplitude and the signal-to-noise ratio (S/N) is 10 log $(A_i^2/2\sigma_i^2)$. The optimal detector is the likelihood ratio

$$L = \prod_{i=1}^{n}\left[p(x_i|A_i)/p(x_i|A_i = 0)\right], \tag{2}$$

where $x_1, \ldots, x_n$ are n independent samples. A target is declared when L is greater than the threshold which determines the probability of false alarm (P_{fa}). Using a small signal approximation, we can show that the likelihood test is equivalent to comparing

$$\sum_{i=1}^{n} A_i^2 x_i^2/\sigma_i^4 \tag{3}$$

Manuscript submitted July 30, 1980.

to an appropriate threshold. If the noise samples are identically distributed ($\sigma_i = \sigma$ for all i) and the $\{A_i\}$ are set to one, then (3) reduces to

$$\sum_{i=1}^{n} x_i^2 > K\sigma^2 . \tag{4}$$

Since σ^2 is usually unknown, σ^2 must be estimated. The implementation of (4) is the cell-averaging CFAR (constant false alarm rate) detector discussed by Finn and Johnson [1] and shown in Fig. 1. This detector uses the shift registers (SR) to save the last N samples in each range cell, integrates the samples in a moving window (MW), and then performs the thresholding (CFAR) function.

To investigate the effects of jamming on this detector, let us consider the return signal and jammer powers, P_S and P_J respectively. If we define S by

$$P_S = SG_S^2 , \tag{5}$$

where G_S is the radar-antenna power gain (one way) in the direction of the target divided by the midbeam gain, and we define J by

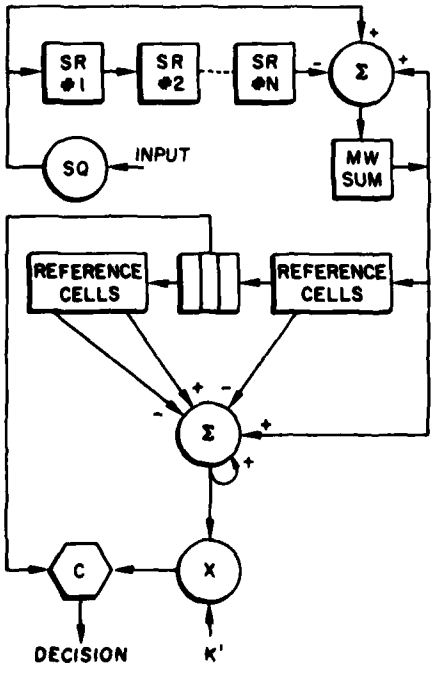

Fig. 1 -- Cell-average CFAR detector: SR is a shift register, MW is a moving window, and C is a comparator

$$P_J = JG_J \,, \tag{6}$$

where G_J is the radar-antenna power gain in the direction of the jammer divided by the mid-beam gain, S and J represent received signal and jamming powers independent of the antenna geometry with respect to the target and jammer. Using these normalized powers and letting P_n be the received thermal noise power, we can write

$$\frac{S}{N} = \frac{SG_S^2}{P_n + JG_J} \,. \tag{7}$$

Consider a hypothetical 200 n. mi. radar that has 16 pulses on target. From Robertson [2], a S/N = 4 dB per pulse is required to achieve a probability of detection (P_D) of 0.9 and a P_{fa} of 10^{-6}. Thus, at a range of 100 n. mi., S/N = 16 dB per pulse, a value large enough so that detections can be declared on a single pulse. Now consider the target-jammer separation with respect to the sin θ/θ antenna pattern shown in Fig. 2. The jammer is in a null of the antenna pattern, and the signal power is only reduced a few dB; i.e., $G_S \gg G_J$. Consequently, as shown in Fig. 3, the S/N (given by (7)) is large for one of the pulses as the antenna beam sweeps by the target, and theoretically the target can be detected. However, if the cell-averaging CFAR detector is used, the target will not be detected because the average signal power is small in comparison to the average jamming power.

For example, if the geometry in Fig. 2 is used, if S/P_n = 20 dB, and if S/J = -20 dB, the S/N ratios in Table 1 are obtained. Examination of Table 1 reveals that the highest S/N (13.6 dB) is obtained when the target is located approximately 8 pulses before the beam center. If no integration were performed (i.e., if the decision were made on a single-pulse basis), a S/N = 13.6 dB would yield a $P_D > 0.9$. However, if the cell-average CFAR detector is used, the equivalent input S/N is given by

$$\left(\frac{S}{N}\right)_{CA} = \frac{\sum_{i=1}^{n} P_S(i)}{\sum_{i=1}^{n} \left[P_n(i) + P_J(i)\right]} \,. \tag{8}$$

For the data in Table 1, the greatest $(S/N)_{CA}$ is 0.38 (-4.2 dB), and this value is obtained by integrating the 16 pulses from -14 to 1. From Robertson [2] (assuming there is no difference between linear and square-law detectors), the P_D corresponding to n = 16 and S/N = -4.2 dB is less than 0.05.

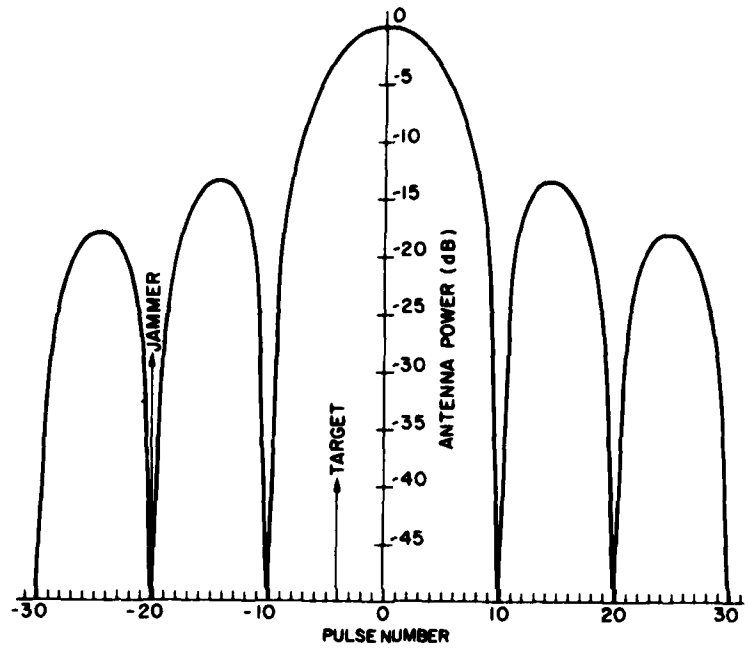

Fig. 2 — Target-jammer geometry with respect to antenna pattern

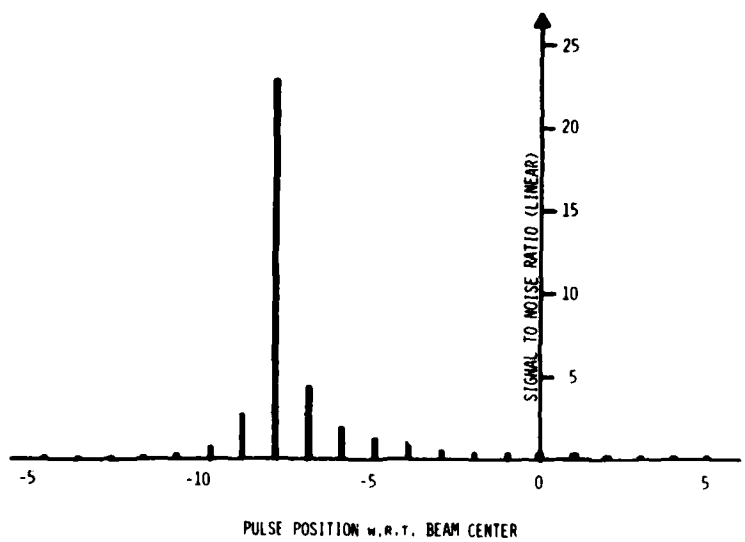

Fig. 3 — Signal-to-noise ratio per pulse as antenna sweeps over target

Table 1 — S/N Per Pulse

Pulse Position w.r.t. Beam Center	S/N (dB)
-15	-21.5
-14	-17.0
-13	-14.0
-12	-10.1
-11	- 6.1
-10	- 1.2
- 9	4.4
- 8	13.6
- 7	6.4
- 6	2.8
- 5	0.9
- 4	- 1.1
- 3	- 2.5
- 2	- 4.0
- 1	- 4.5
0	- 5.0
1	- 6.0
2	- 7.0
3	- 8.0
4	- 9.0
5	-10.0

On the other hand, if the test cell is normalized (divided) by the average of the reference cells and then integrated as in Fig. 4, the effective S/N for this ratio detector is given by

$$\left(\frac{S}{N}\right)_R = \frac{1}{n}\sum_{i=1}^{n}\frac{P_S(i)}{P_n(i) + P_J(i)} . \tag{9}$$

For the data in Table 1, the greatest $(S/N)_R$ is 2.32 (3.7 dB); this value is obtained by integrating the 16 pulses from -11 to 4. If Robertson's curves [2] are used (although they were derived for a linear detector, they will yield approximate results for the ratio detector), the $P_D = 0.9$.

The reason the ratio detector is very effective can be understood if we reexamine (3): since σ_i is unknown and varying from pulse to pulse, σ_i cannot be placed on the right-hand side of the inequality as in (4). It can readily be shown that no uniformly most powerful test exists (i.e., the optimal test depends on specific values of $\{\sigma_i\}$). A logical way of pro-

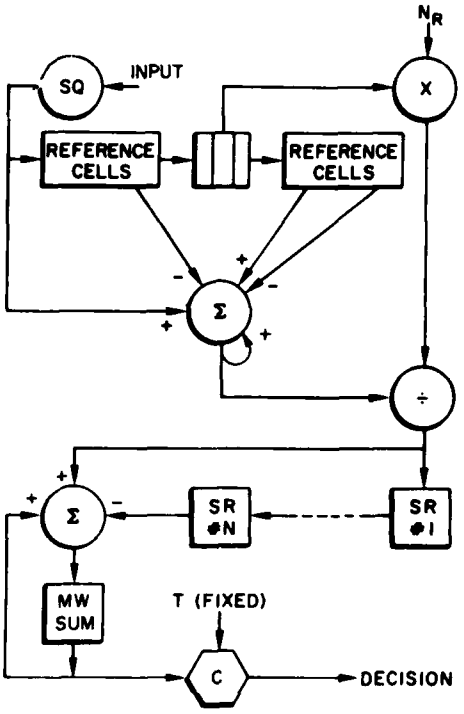

Fig. 4 -- Ratio detector: SR is a shift register, MW is a moving window, NR is the number of reference cells, and C is a comparator

ceeding is to use the generalized likelihood ratio test of Van Trees [3], replacing the unknown parameters with an estimate. Thus, it can be seen that Fig. 4 is just an implementation of the generalized likelihood ratio detector. The detector output is

$$\sum_{i=1}^{n} \frac{x_i^2(j)}{\frac{1}{2m}\sum_{k=1}^{m}\left[x_i^2(j+1+k)+x_i^2(j-1-k)\right]}, \tag{10}$$

where $x_i(j)$ is the ith envelope detected pulse in the jth range cell and $N_R = 2m$ is the number of reference cells. The denominator is an estimate of σ_i^2 and, essentially, the detector sums signal-to-noise power ratios.

It should be noted that the square-law detector should be used rather than the linear detector, since the problem is equivalent to the collapsing loss problem. However, instead of the signal disappearing for many pulses, the noise (jamming) increases for many pulses. Since it has been shown by Trunk [4] that the collapsing loss is much smaller for a square-law detector, this detector should be used.

DETECTOR CALCULATIONS

To compare the performance of the ratio detector with that of the cell-averaging CFAR, we generated P_D curves using a Monte Carlo simulation. First, by use of the concept of importance sampling (see appendix), threshold curves were generated; they are shown in Fig. 5. The P_D curves for the two detectors in thermal noise were found by a straightforward simulation and are shown in Figs. 6 and 7. The ratio detector requires 0.2 dB more signal to yield the same P_D as the cell-average CFAR.

The performance of the detectors in sidelobe jamming is quite complicated; it is a function of S/P_n, S/J, and the angular separation of target and jammer. Curves of P_D versus target-jammer separation in beamwidths for $S/J = -20$ dB and $S/P_n = 16$ and 20 dB are shown in Fig. 8. We calculate the P_D by finding the maximum detector outputs as the beam sweeps over the target and then comparing these maximum values to the appropriate thresholds. In all cases, the performance of the ratio detector is better than that of the cell-average CFAR. Also, the greater the value of S/P_n, the greater the performance difference.

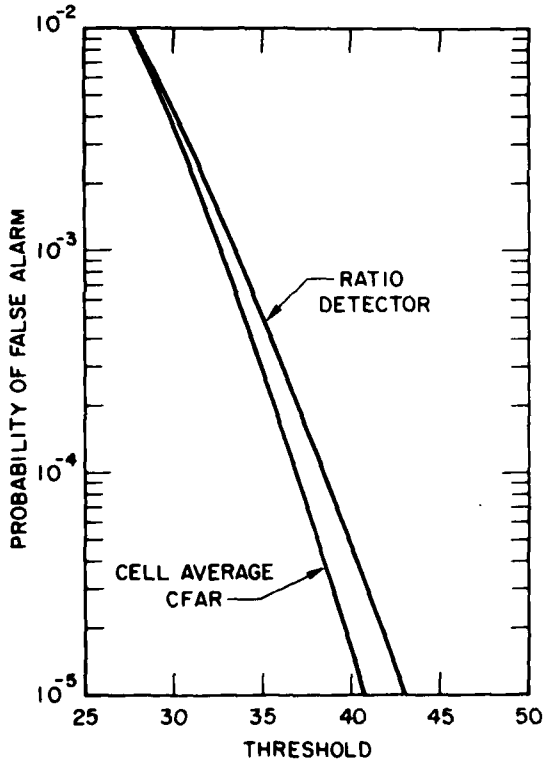

Fig. 5 — Threshold values for cell-average CFAR and ratio detectors

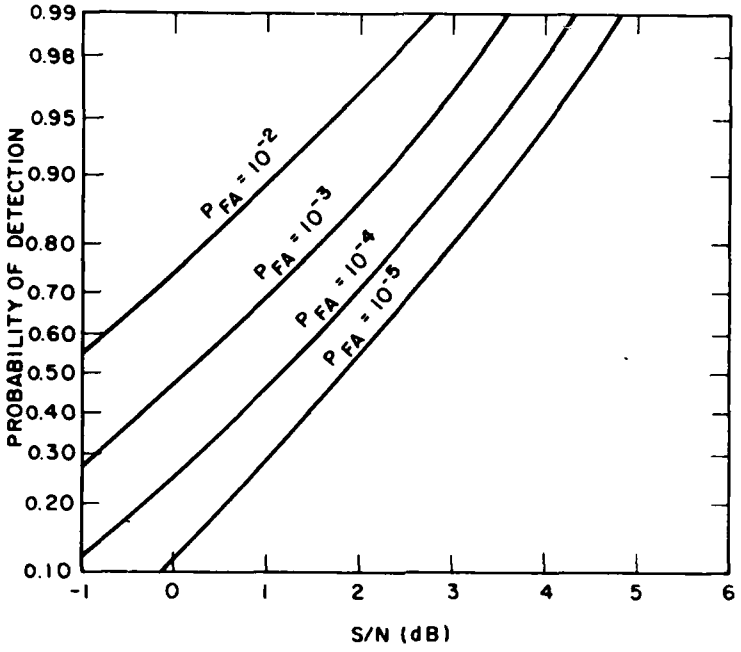

Fig. 6 — Probability-of-detection curves for cell-average CFAR detector

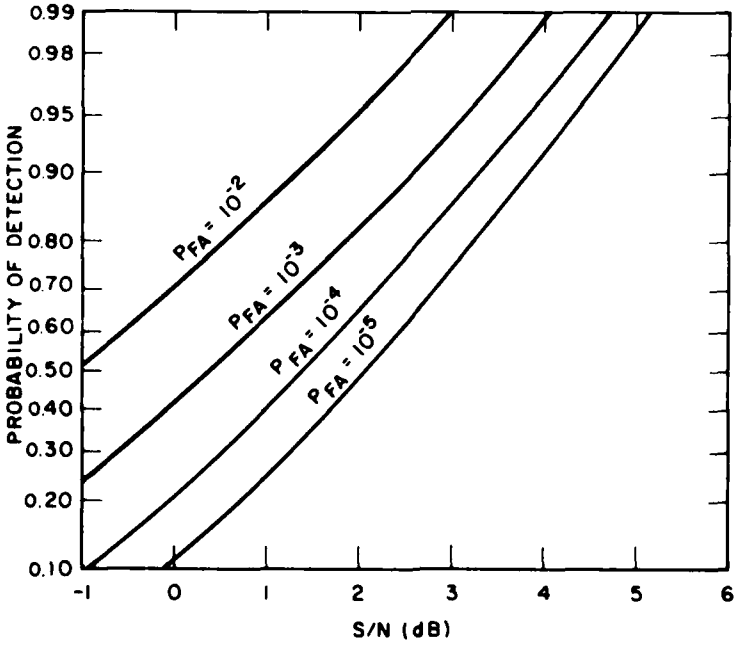

Fig. 7 — Probability-of-detection curves for ratio detector

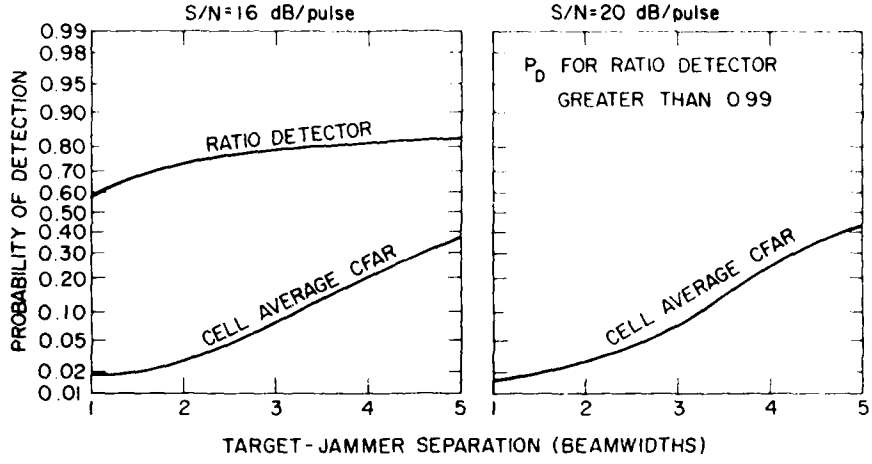

Fig. 8 — Probability-of-detection curves for detectors in sidelobe jamming: $S/J = -20$ dB and $P_{fa} = 10^{-6}$

ANGULAR ESTIMATES

When a target is detected with the ratio detector (with the jamming being in an antenna null), it is impossible to obtain an accurate azimuth estimate. Specifically, for very high S/P_n and very low S/J the azimuth error is uniformly distributed in an interval approximating the beamwidth. Also, the azimuth estimates are not independent from scan to scan, because the estimate is essentially the midbeam antenna position when the jammer is in a null and the target is in the main beam. Thus, the azimuth estimates follow the jammer movement (with a large bias) until the target-jammer separation changes so that the target is detected when the jammer is in a different antenna null. At this time, the estimate will change by a beamwidth.

The type of behavior one obtains is illustrated in Fig. 9. In this example, the jammer is initially at 90° and is moving 0.3°/scan, the target is initially at 87° and is moving −0.4°/scan, and the nulls are separated by 3°. The estimated azimuth lags the jammer by one beamwidth initially, later by two beamwidths, and finally by three beamwidths. Special care must be taken to incorporate this type of behavior into the tracking algorithm, since the angle estimates are uniformly distributed about the true azimuth and will occasionally have discontinuities of the order of a beamwidth, whereas normally the azimuth estimates are assumed to be Gaussian distributed.

EXPERIMENTAL RESULTS

Theoretically, the performance of the ratio detector is much better than that of the cell-average CFAR. Consequently, it was decided to compare these detectors using recorded data. Specifically, two S-band TWTs (located on building #5 and on the north gatehouse at bearings of approximately 167° and 185°, respectively, from the radar) were used to jam

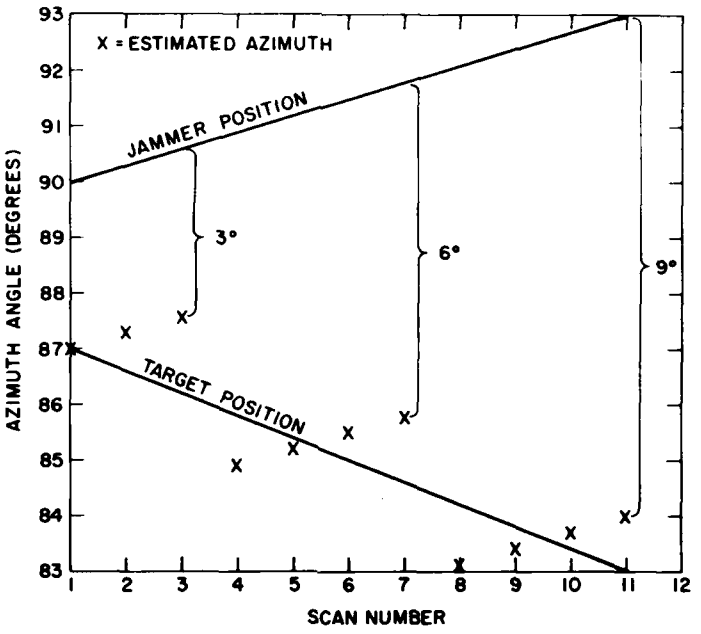

Fig. 9 — Azimuth estimate with respect to target-jammer geometry

the SPS-39 radar at CBD. A recording system recorded 65532 eight-bit numbers corresponding to a designated R-θ region as the radar rotated. After the 65532 data words were accumulated, the data were dumped on to magnetic tape in approximately 1.5 s. Thus, the system was ready to record the next scan of the designated R-θ region by the time the beam next entered the region.

The data presented in this paper were taken on May 28, 1980. Data were recorded from two different R-θ regions. The first region started at a range of 50 n. mi. and an azimuth of 115° and consisted of 64 range cells for each of 1024 transmitted pulses. The second region again started at a range of 50 n. mi. and an azimuth of 115° but consisted of 128 range cells for each of 512 transmitted pulses. Since the radar PRF was 500 pps and the radar scan rate was 8 s, the first region covered 90° of azimuth and the second covered 45°. For each region, three different sets of jamming data were recorded:

- The jammer at the north gatehouse was set at maximum attenuation and the envelope-detected samples were recorded as the jamming power (on building #5) was reduced in 6-dB steps.

- The jammer at building #5 was set at maximum attenuation and data were recorded as the jamming power at the north gatehouse was reduced in 6-dB steps.

- The jammers were set to approximately the same power and data were recorded as both jammers were attenuated in 6-dB increments.

Some typical recorded data from region 1 are plotted in Fig. 10 and Figs. 11*a* to 11*l*, where the returned power is found by averaging the 64 range samples available. Since the radar was not transmitting, these plots represent the sum of the average thermal noise and jamming powers as a function of scanning angle. If, in the denominator of Eq. (7) (i.e., $P_n + JG_J$), $JG_J \gg P_n$, the plots represent the antenna gain G_J. Thus, by noting that the average noise level in Fig. 10 is 18 dB, we can infer that the mainbeam jamming (with no attenuation) is 70 dB above the thermal noise. Since there are several local minima 15 to 20 dB below adjacent maxima, one would expect the ratio detector to have a higher probability of detection than the cell-average CFAR.

To compare the two detectors, signal is added to the recorded data to simulate the presence of a target. For example, since there are approximately 21 pulses between the 3-dB antenna points, signal can be introduced into any range cell by

$$x_i^2 = \left[A \frac{\sin K(j - i)}{K(j - i)} + Z_i \cos \theta_i \right]^2 + (Z_i \sin \theta_i)^2 , \tag{11}$$

where A is the signal amplitude, $K = 1.3916/10.5$, j is the indexed azimuth location of the target, and z_i is the ith recorded pulse (PRF) in the range cell. The signal is first introduced into the ninth range cell. Then, this signal and the jamming signals in the eight range cells on either side of the ninth cell are put into the cell-average CFAR (Fig. 1) and the ratio detector (Fig. 4) and any detections are noted. This calculation is repeated for the target in the 13, 17, 21, ..., 49, and 53 cells, yielding 12 detection opportunities. The signal level A for each azimuth is adaptively adjusted so that the number of detections made by the ratio detector is between 9 and 11 for region 1.* Then the number of detections made by both detectors is recorded; this is plotted in Fig. 12. A comparison of the two detection

*If the signal strength is greater than 255, this value exceeds the dynamic range of the recorded data and consequently the number of detections is arbitrarily set to zero for both detectors.

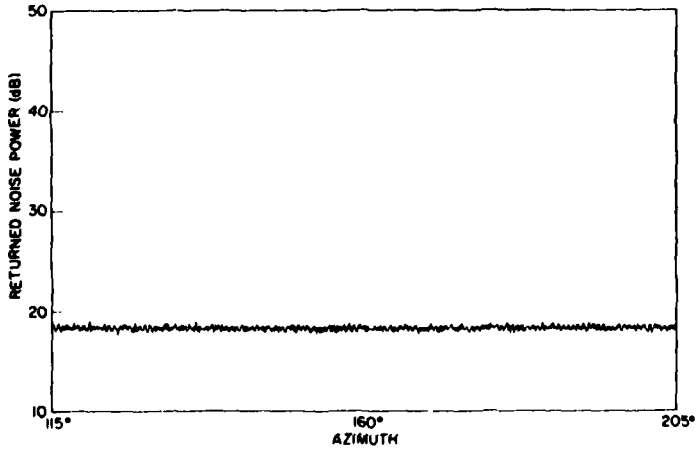

Fig. 10 — Returned noise power vs radar azimuth angle

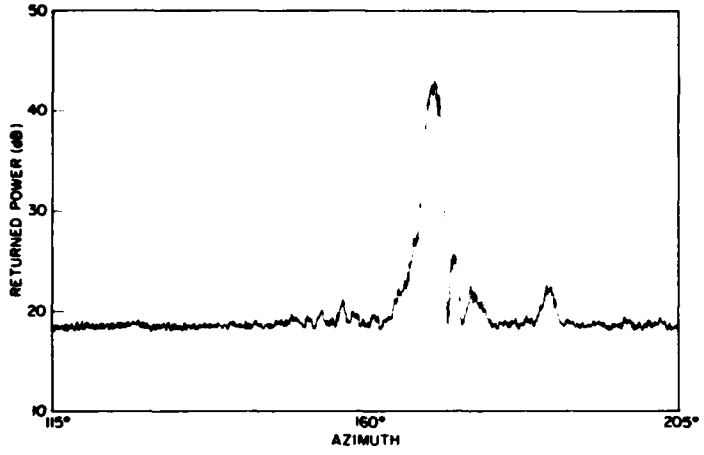

(a) Attenuations Bldg. #5 = 57 dB and NGH = Max

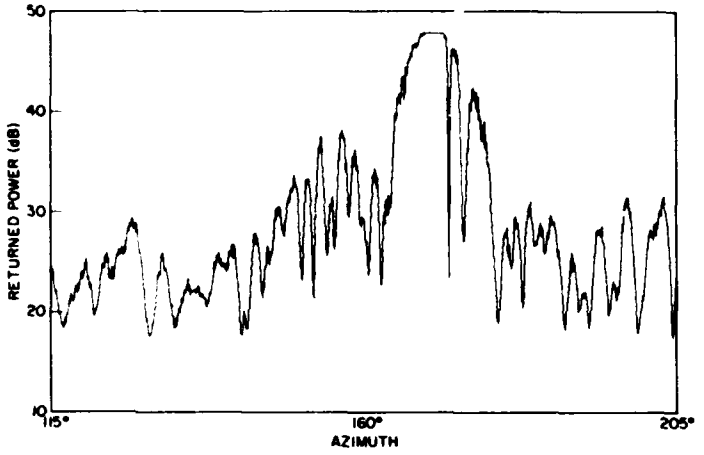

(c) Attenuations Bldg. #5 = 33 dB and NGH = Max

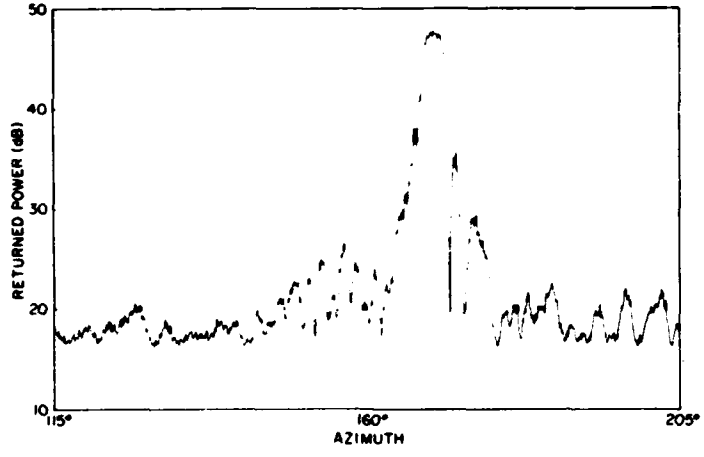

(b) Attenuations Bldg. #5 = 45 dB and NGH = Max

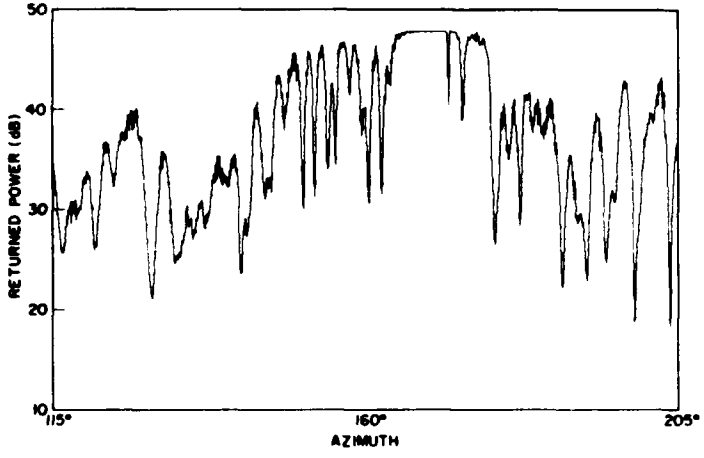

(d) Attenuations Bldg. #5 = 21 dB and NGH = Max

Fig. 11 — Returned jamming plus noise power vs radar azimuth angle. The jamming attenuations for building #5 and the north gatehouse (NGH) are given for each case.

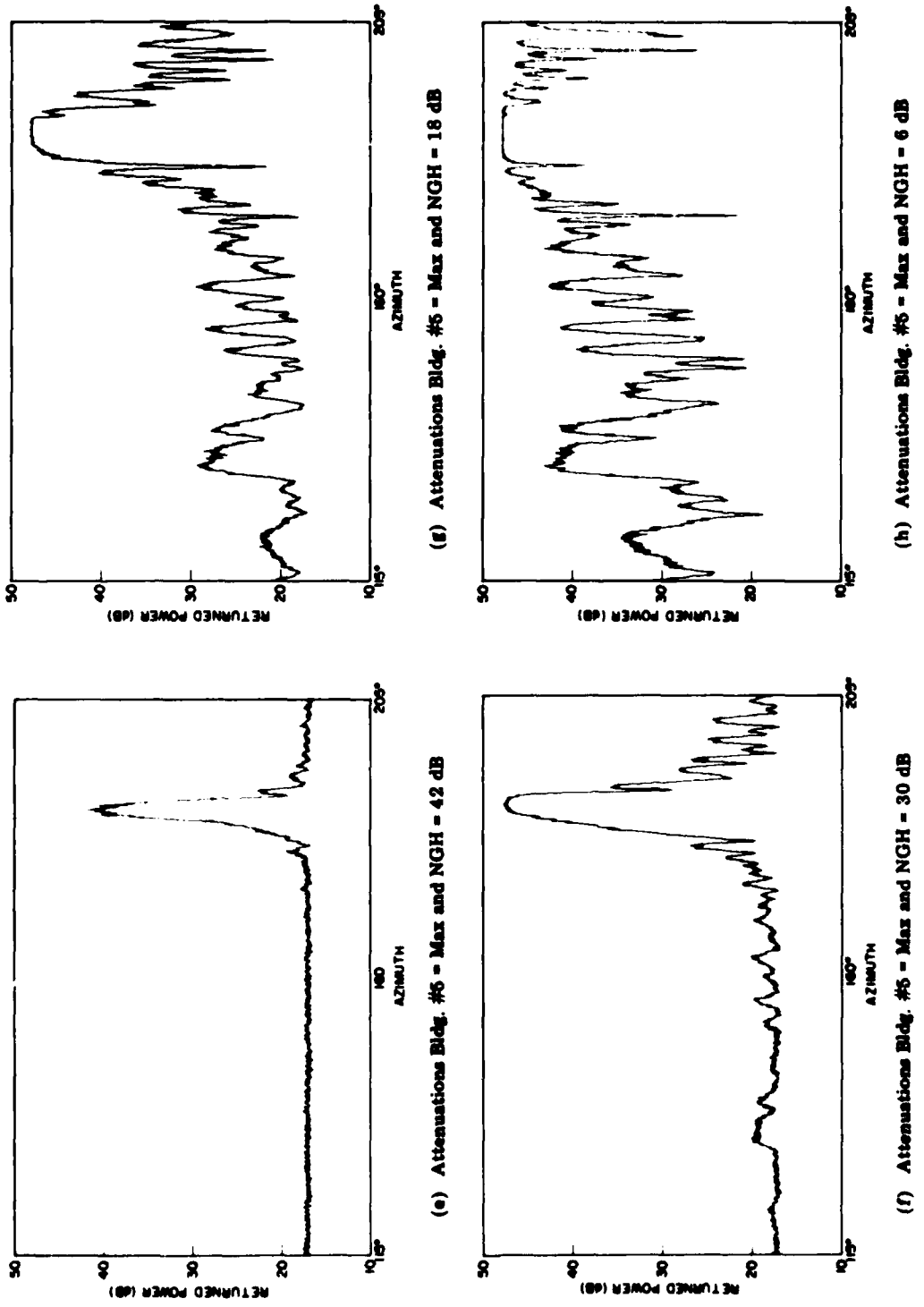

(e) Attenuations Bldg. #5 = Max and NGH = 42 dB

(f) Attenuations Bldg. #5 = Max and NGH = 30 dB

(g) Attenuations Bldg. #5 = Max and NGH = 18 dB

(h) Attenuations Bldg. #5 = Max and NGH = 6 dB

Fig. 11 -- Returned jamming plus noise power vs radar azimuth angle (Continued)

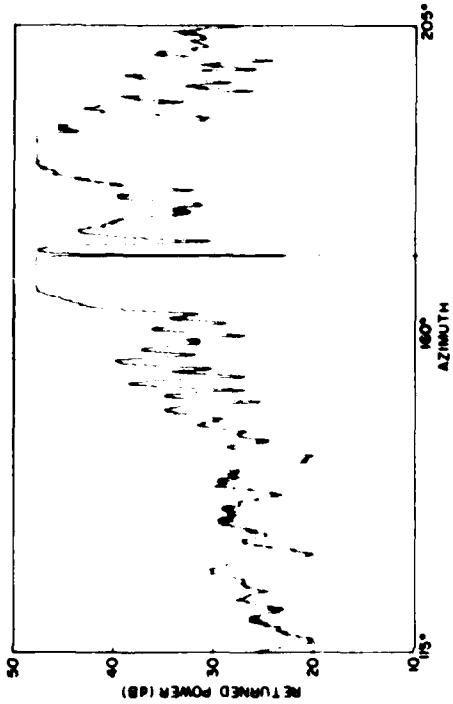

(k) Attenuations Bldg. #5 = 33 dB and NGH = 18 dB

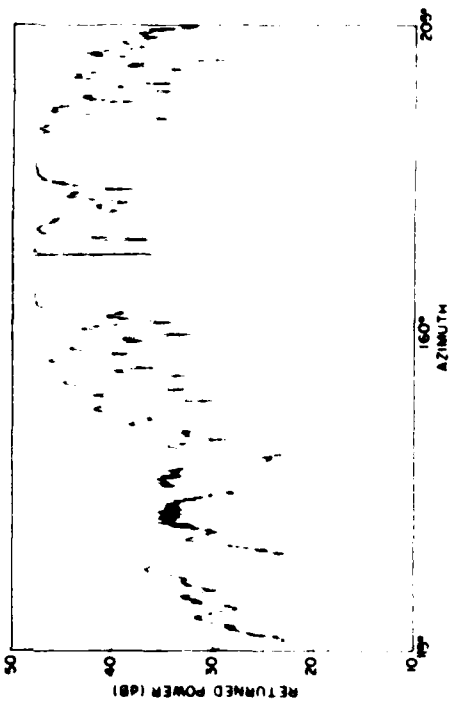

(l) Attenuations Bldg. #5 = 27 dB and NGH = 12 dB

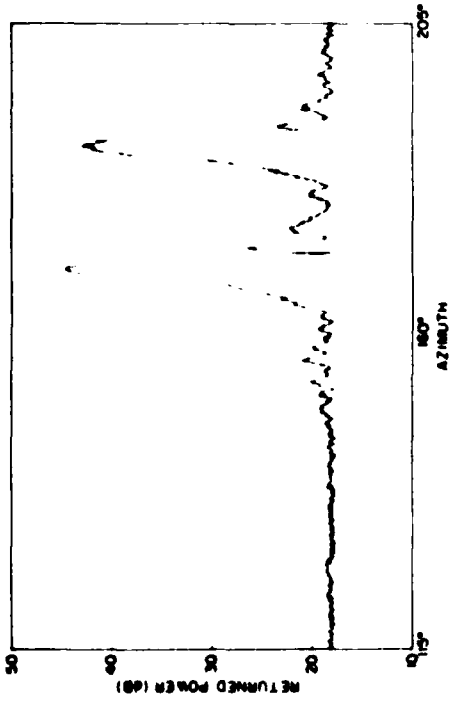

(i) Attenuations Bldg. #5 = 57 dB and NGH = 42 dB

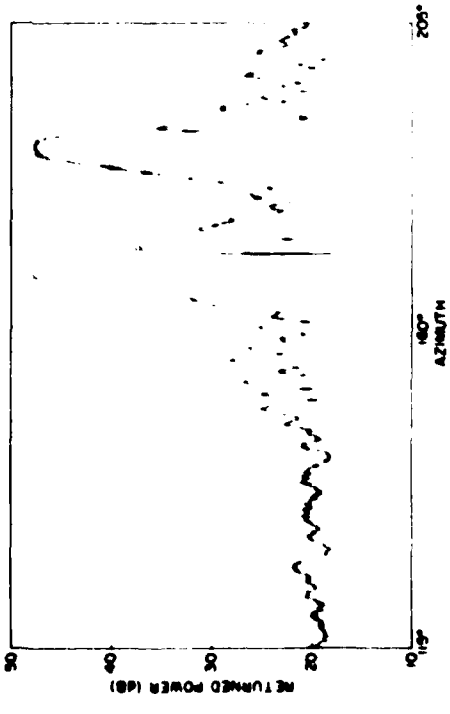

(j) Attenuations Bldg. #5 = 45 dB and NGH = 30 dB

Fig. 11 – Returned jamming plus noise power vs radar azimuth angle (Continued)

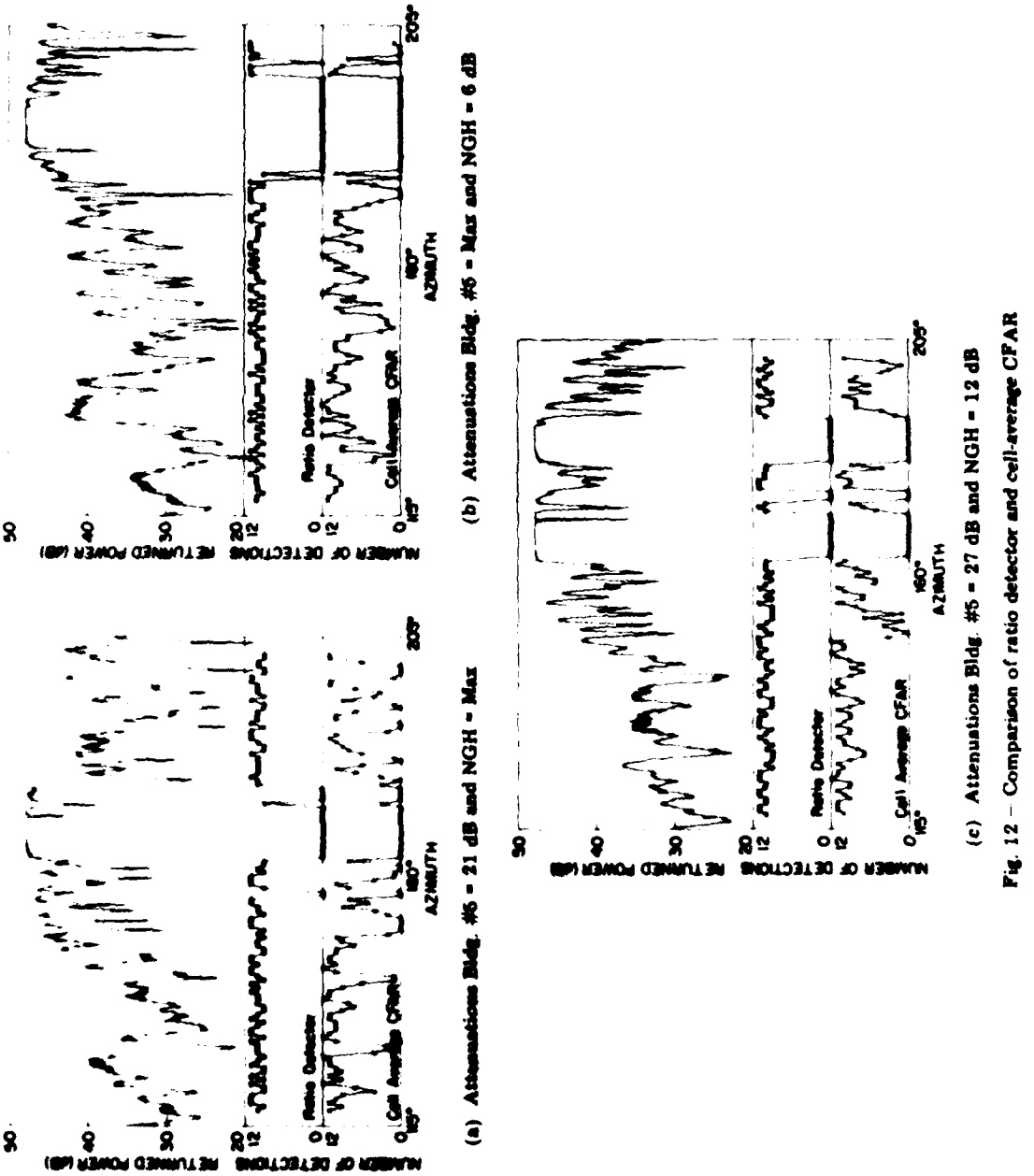

(a) Attenuations Bldg. #6 = 21 dB and NGH = Max

(b) Attenuations Bldg. #6 = Max and NGH = 6 dB

(c) Attenuations Bldg. #5 = 27 dB and NGH = 12 dB

Fig. 12 – Comparison of ratio detector and cell-average CFAR

curves shows that there are several instances where the probability of detection of the ratio detector is over 80%, whereas that of the cell-average CFAR is zero. Furthermore, these large differences occur when there is a very sharp and deep null in the antenna pattern.

Table 2 was generated to try to give a number which describes the advantage of the ratio detector over the cell-average CFAR. Here, the overall probability of detection arrived at by averaging over all azimuths indicates less than a 1-dB advantage for the ratio detector. However, this does not tell the whole story. If one refers to Fig. 13, which gives the histogram of the number of detections for the first entry in Table 2, one sees that 14% of the time the cell-average CFAR did not detect the target even once, whereas the average number of detections was 10 for the ratio detector. Thus, 14% of the time the ratio detector was more than 4 dB better than the cell-average CFAR.

Table 2

Jamming Attenuation (dB)		Detection Probabilities		Difference (dB)
Building #5	North Gatehouse	Ratio	C.A. CFAR	
21	Max	0.834	0.556	1.0
Max	6	0.836	0.642	0.7
27	12	0.841	0.686	0.5
Max	Max	0.797	0.760	0.1

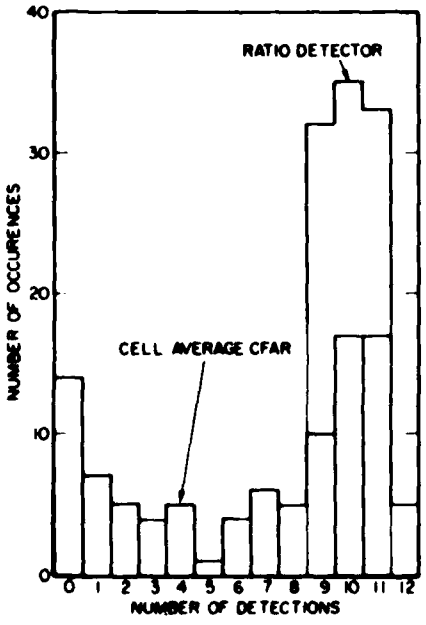

Fig. 13 — Histogram of number of detections at each azimuth for the ratio detector and cell-average CFAR

CONCLUSIONS

The problem of designing an automatic detector in a sidelobe-jamming environment has been considered, and it has been shown that a ratio detector has better performance than the cell-average CFAR detector. The performance of the detectors is essentially equivalent in thermal noise. However, in sidelobe jamming with S/P = 20 dB and S/J = - 20 dB, theoretically the P_D for the ratio detector is greater than 0.99, whereas the P_D for the cell-average CFAR detector ranges between 0.02 and 0.42, depending on target-jammer angular separation. Furthermore, experiments using recorded jamming data confirm the advantages of the ratio detector. Specifically, although the advantage of the ratio detector (averaged over all azimuths) is less than 1 dB, more than a 4-dB advantage occurs about 14% of the time. Also, it is worth noting that the ratio detector will have a performance advantage in jamming when pulse-to-pulse frequency diversity is employed. This is because, when frequency diversity is used, the antenna gain in the direction of the jammer will change and, correspondingly, the received jamming power will vary from pulse to pulse.

The main disadvantage of the ratio detector is that it will detect single-pulse interference. However, one can probably obtain performance equivalent to that of the ratio detector by using two types of detectors, the normal cell-averaging CFAR and an M out of N detector where $M = N = 2$ regardless of the number of pulses in the beamwidth. This possibility will be investigated in future work.

ACKNOWLEDGMENTS

I wish to thank D. Queen, J. Alter, A. March, D. Hut, and M. Siegert for obtaining the jamming data and J. Wilson for helping me with various computer programs.

REFERENCES

1. H. M. Finn and R. S. Johnson, RCA Review **29**, 414-464 (1968).
2. G. H. Robertson, Bell Syst. Tech. J. **46**, 755-774 (1967).
3. H. L. Van Trees, *Detection, Estimation, and Modulation Theory, Part 1*, Wiley, New York, 1968.
4. G. V. Trunk, Proc. IEEE **60**, 743-744 (1972).

Appendix

IMPORTANCE SAMPLING

Although Monte Carlo simulations have been used for many years to calculate P_D curves, they have not been used to calculate P_{fa} curves because of the enormous number of repetitions usually required, approximately $10/P_{fa}$. However this difficulty can be overcome by the use of importance sampling. The fundamental principle of the importance-sampling technique is a modification of the probabilities that govern the outcome of the basic experiment of the simulation so that the event of interest (the false alarm) occurs more frequently. We then compensate for this distortion by weighting each event by the ratio of the probability that this specific event would have occurred if the true probabilities had been used in the simulation to the probability that this same event would occur with the distorted probabilities. Consequently, by proper choice of the distorted probabilities the number of repetitions can be reduced greatly. For instance, the mean of a function $Q(x)$ is given by

$$E\{Q(x)\} = \int Q(x)\, dP(x) ,$$

where $P(x)$ is the distribution of x. We can estimate the mean of $Q(x)$ by selecting M independent samples x_i from $P(x)$ and associating the probability $1/M$ with each event. The $E\ Q(x)$ can be estimated by

$$\frac{1}{M} \sum_{i=1}^{M} Q(x_i) . \tag{A1}$$

The importance-sampling technique uses the Radon-Nikodym derivative to express the mean value of $Q(x)$ by

$$E\{Q(x)\} = \int Q(x) \frac{dP(x)}{dG(x)}\, dG(x) ,$$

where $G(x)$ is a distribution function. We can now estimate the mean $E\{Q(x)\}$ by selecting M independent samples from $G(x)$ and associating the probability $dP(x_i)/MdG(x_i)$ with each event $Q(x_i)$. Thus $E\{Q(x)\}$ is estimated by

$$\frac{1}{M}\sum_{i=1}^{M} Q(x_i)\frac{dP(x_i)}{dG(x_i)}. \tag{A2}$$

Since (A1) and (A2) are both unbiased estimates of $Q(x)$, it is possible to select $G(x)$ so that the variance of (A2) is less than the variance of (A1).

In our problem of determining the threshold T for a desired P_{fa} for the ratio detector, it is necessary to estimate the distribution curve

$$P(Z \leqslant T) = 1 - P_{fa}\ , \tag{A3}$$

where

$$Z = \sum_{i=1}^{n} \frac{x_i^2(j)}{\frac{1}{2m}\sum_{k=1}^{m}\left[x_i^2(j+1+k) + x_i^2(j-1-k)\right]} \tag{A4}$$

and the $x_i(k)$ are independent Rayleigh variables. The straightforward way of generating the squared samples is by

$$x_i^2(k) = \sigma^2(-2\ln U_{ik}) \quad \text{for all } k\ , \tag{A5}$$

where U_{ik} are independent random numbers uniformly distributed on the interval (0, 1). To estimate (A3), we form M independent ratios $\{Z_J, J = 1, ..., M\}$ using (A4) and (A5); the estimated distribution is

$$P(Z \geqslant T) = \frac{1}{M}\sum_{J=1}^{M}\delta_J\ ,$$

where

$$\delta_J = 1, \quad Z_J \geqslant T\ ,$$

$$= 0, \quad Z_J < T\ .$$

Importance sampling differs from the previous procedure by generating samples using

$$x_i^2(j) = \alpha^2(-2 \ln U_{ij}) \tag{A6}$$

and

$$x_i^2(k) = \sigma^2(-2 \ln U_{ik}) \qquad k \neq j\,, \tag{A7}$$

where $\alpha > \sigma$, a technique which yields more false alarms. From (A4), (A6), and (A7), M ratios Z_J are generated. Then the estimated distribution is

$$P(Z \geq T) = \frac{1}{M} \sum_{J=1}^{M} \delta_J P_J\,,$$

where

$$\delta_J = 1, \quad Z_J \geq T\,,$$

$$= 0, \quad Z_J < T\,,$$

and

$$P_J = \left(\frac{\alpha}{\sigma}\right)^{2N} \exp\left[(1/2\alpha^2 - 1/2\sigma^2) \sum_{i=1}^{N} x_i^2(j)\right]$$

Typically, $M = 10^4$ cases are used to estimate thresholds for $P_{fa} = 10^{-6}$.